AMERICAN SOCIETY FOR MICROBIOLOGY | mSphere®

RESEARCH ARTICLE
Host-Microbe Biology

Differential Ability of Pandemic and Seasonal H1N1 Influenza A Viruses To Alter the Function of Human Neutrophils

Natalia Malachowa,[a] Brett Freedman,[a] Daniel E. Sturdevant,[b] Scott D. Kobayashi,[a] Vinod Nair,[c] Friederike Feldmann,[d] Tregei Starr,[a] Olivia Steele-Mortimer,[a] John C. Kash,[e] Jeffery K. Taubenberger,[e] Heinz Feldmann,[f] Frank R. DeLeo[a]

[a]Laboratory of Bacteriology, Rocky Mountain Laboratories, National Institute of Allergy and Infectious Diseases, National Institutes of Health, Hamilton, Montana, USA

[b]Genomics Unit, Research Technologies Section, Rocky Mountain Laboratories, National Institute of Allergy and Infectious Diseases, National Institutes of Health, Hamilton, Montana, USA

[c]Electron Microscopy Unit, Research Technologies Section, Rocky Mountain Laboratories, National Institute of Allergy and Infectious Diseases, National Institutes of Health, Hamilton, Montana, USA

[d]Rocky Mountain Veterinary Branch, Rocky Mountain Laboratories, National Institute of Allergy and Infectious Diseases, National Institutes of Health, Hamilton, Montana, USA

[e]Laboratory of Infectious Diseases, National Institute of Allergy and Infectious Diseases, National Institutes of Health, Bethesda, Maryland, USA

[f]Laboratory of Virology, Rocky Mountain Laboratories, National Institute of Allergy and Infectious Diseases, National Institutes of Health, Hamilton, Montana, USA

ABSTRACT Neutrophils are essential cells of host innate immunity. Although the role of neutrophils in defense against bacterial and fungal infections is well characterized, there is a relative paucity of information about their role against viral infections. Influenza A virus (IAV) infection can be associated with secondary bacterial coinfection, and it has long been posited that the ability of IAV to alter normal neutrophil function predisposes individuals to secondary bacterial infections. To better understand this phenomenon, we evaluated the interaction of pandemic or seasonal H1N1 IAV with human neutrophils isolated from healthy persons. These viruses were ingested by human neutrophils and elicited changes in neutrophil gene expression that are consistent with an interferon-mediated immune response. The viability of neutrophils following coculture with either pandemic or seasonal H1N1 IAV was similar for up to 18 h of culture. Notably, neutrophil exposure to seasonal (but not pandemic) IAV primed these leukocytes for enhanced functions, including production of reactive oxygen species and bactericidal activity. Taken together, our results are at variance with the universal idea that IAV impairs neutrophil function directly to predispose individuals to secondary bacterial infections. Rather, we suggest that some strains of IAV prime neutrophils for enhanced bacterial clearance.

IMPORTANCE A long-standing notion is that IAV inhibits normal neutrophil function and thereby predisposes individuals to secondary bacterial infections. Here we report that seasonal H1N1 IAV primes human neutrophils for enhanced killing of *Staphylococcus aureus*. Moreover, we provide a comprehensive view of the changes in neutrophil gene expression during interaction with seasonal or pandemic IAV and report how these changes relate to functions such as bactericidal activity. This study expands our knowledge of IAV interactions with human neutrophils.

KEYWORDS H1N1, *Staphylococcus aureus*, immune response, influenza A virus, neutrophils

Influenza A virus (IAV) remains a common cause of human infections worldwide. The Centers for Disease Control and Prevention estimates that influenza and influenza-related illnesses have accounted for 12,000 to 56,000 deaths in the United States

Received 30 November 2017 **Accepted** 4 December 2017 **Published** 3 January 2018

Citation Malachowa N, Freedman B, Sturdevant DE, Kobayashi SD, Nair V, Feldmann F, Starr T, Steele-Mortimer O, Kash JC, Taubenberger JK, Feldmann H, DeLeo FR. 2018. Differential ability of pandemic and seasonal H1N1 influenza A viruses to alter the function of human neutrophils. mSphere 3:e00567-17. https://doi.org/10.1128/mSphereDirect.00567-17.

Editor Michael J. Imperiale, University of Michigan—Ann Arbor

Address correspondence to Frank R. DeLeo, fdeleo@niaid.nih.gov.

Solicited external reviewers: Al Jesaitis, Montana State University; Jay Kolls, Tulane School of Medicine.

This paper was submitted via the mSphereDirect™ pathway.

annually since 2010 (1). Importantly, the vast majority of these deaths are associated with or caused by secondary bacterial infections (2–5). IAV belongs to the *Orthomyxoviridae* family of RNA viruses, which are characterized by relatively high mutation rates and reassortment of genetic material. Such antigenic drift and shift promotes the emergence of new IAV variants and viruses and subsequently leads to annual epidemics or recurrent pandemics (6). One of the most recent influenza pandemics was caused by swine origin H1N1 IAV (7). As with previous IAV pandemics, bacterial coinfections contributed to morbidity and mortality during the 2009 H1N1 IAV pandemic (2, 4). *Streptococcus pneumoniae*, *Streptococcus pyogenes*, *Haemophilus influenzae*, and *Staphylococcus aureus* were among the most prevalent bacteria recovered from individuals with antecedent IAV infections (8, 9). In a recent retrospective study, Shah et al. demonstrated that bacterial coinfections remain a problem among patients admitted to intensive care units with severe H1N1 influenza virus infection (10). Patients with bacterial coinfections had an ~14% higher mortality rate and nearly double the length of hospital stay (10). *S. aureus* was the most prevalent bacterial species and accounted for 36.5% of all bacterial coinfections in that study (10).

IAV infects epithelial cells of the respiratory tract, where it can replicate and produce progeny virions. Epithelial cells orchestrate the pulmonary inflammatory response by producing numerous molecules that cause an influx of neutrophils and monocytes to the site of infection (11). Infections with pandemic H1N1 A/Mexico/4108/2009 (Mex09) IAV produce more severe upper and lower respiratory tract pathology than those caused by seasonal H1N1 A/Kawasaki/UTK-4/2009 (Kaw09) IAV in nonhuman primate infection models (12–14). 2009 pandemic H1N1 IAV strains elicit greater production of cytokines from epithelial cells and trigger greater neutrophil influx into the lung than seasonal IAV strains do (13–15). Inasmuch as neutrophils are essential for defense against bacterial pathogens, there is a seeming disconnect between the increased neutrophil influx into the lung during these IAV infections and the occurrence of secondary bacterial infections. Many previous studies have reported that IAV impairs neutrophil function directly (16–25), and such a phenomenon could explain, in part, host susceptibility to secondary bacterial infections. Here, we tested the notion that differences in clinical symptoms of upper respiratory tract infections caused by these two viruses are linked to their direct effect on neutrophil function and viability.

RESULTS AND DISCUSSION

Neutrophil uptake of IAV. The exact mechanism of IAV binding and/or uptake by neutrophils is incompletely determined, but previous studies indicate that binding of virus to the surface of neutrophils involves sialylated membrane molecules such as CD43, CD45, CDw65, and sialyl Lewis^x (26–28). Using an *in vitro* microarray assay system, Childs et al. demonstrated that Mex09 and Kaw09 differ in host surface receptor binding specificity (29). Pandemic Mex09 can bind α2,3- and α2,6-linked sialic acid receptors, whereas seasonal Kaw09 IAV binds predominantly an α2,6-linked sialic acid receptor (29). We first evaluated the binding and uptake of purified IAV by human neutrophils by using fluorescence microscopy (Fig. 1). IAV particles were associated with human neutrophils within 30 min (Fig. 1A). On the basis of multiple experiments, there was no difference in the ability of Mex09 or Kaw09 to bind neutrophils. Although there was a difference in the percentage of neutrophils that had ingested Mex09 or Kaw09 at 30 min (40.5% $\pm$ 5.7% for Mex09 versus 69.0% $\pm$ 8.3% for Kaw09), it was not statistically significant ($P = 0.07$) (Fig. 1B). Interestingly, ingested IAV was typically found within a membrane-bound vacuole (Fig. 1C), results consistent with studies published in the 1980s (19, 30).

Synthesis of transcripts encoding viral molecules. We next used a real-time quantitative reverse transcriptase PCR (qRT-PCR) approach to evaluate whether neutrophils synthesize transcripts encoding viral proteins. Although neutrophils are terminally differentiated cells, they have the capacity to synthesize new transcripts and proteins, albeit to a limited extent compared to cells that replicate. Following coculture with neutrophils, there was a limited increase in IAV matrix gene transcripts over time,

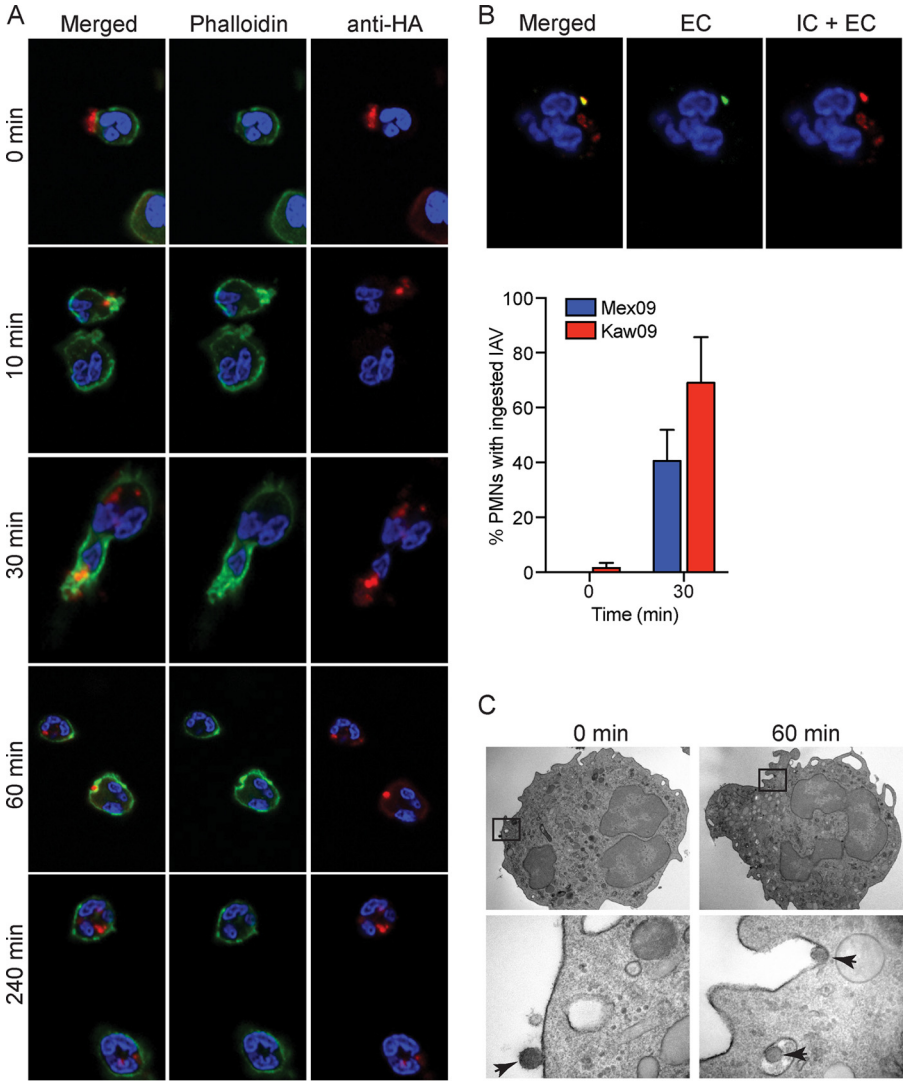

FIG 1 Uptake of IAV by human neutrophils. (A) Purified human neutrophils were cocultured with Kaw09 virus for up to 4 h. Association of virus with neutrophils was monitored by immunofluorescence microscopy. Neutrophil F-actin was detected by labeling with Alexa Fluor 488-conjugated phalloidin (green). IAV was detected with an anti-HA antibody (red). DAPI was used to visualize neutrophil nuclei (blue). (B) Uptake of Mex09 and Kaw09 (each at an MOI of 5) by human PMNs was determined by fluorescence microscopy as described in Materials and Methods. The upper panels are representative images of Kaw09 uptake at 30 min. The left panel is a merged image of the middle and right panels. Particles that stained red only are ingested. The middle panel depicts extracellular (EC) associated viral particles (green). The right panel shows a combination of extracellular and ingested (intracellular [IC]) viral particles (red). The bar graph is a quantitation of the microscopy data. Data are presented as the mean ± the standard error of the mean from three experiments. (C) TEM analysis of Kaw09 uptake by a human neutrophil. Direct magnification in the upper panels is at ×11,000. Each rectangle indicates the area enlarged in the panel below (×98,000). The arrowheads indicate IAV.

especially compared to the increase in viral RNA transcripts in MDCK cells infected at the same multiplicity of infection (MOI) (Fig. 2A). Inasmuch as uptake of IAV by MDCK cells (see Fig. S1 in the supplemental material) was more efficient than that by neutrophils (Fig. 1B), infected MDCK cells were used as a positive control for productive viral replication. Consistent with the limited increase in IAV RNA during coculture with neutrophils, we were unable to detect the production of viral proteins in infected neutrophils (Fig. 2B). These data suggest that there is no productive infection of human neutrophils. These findings are at variance with a previous study by Cassidy et al. (31), who reported that human neutrophils synthesize IAV proteins. It is possible that differences in the sensitivity of protein detection between the two methods—radiola-

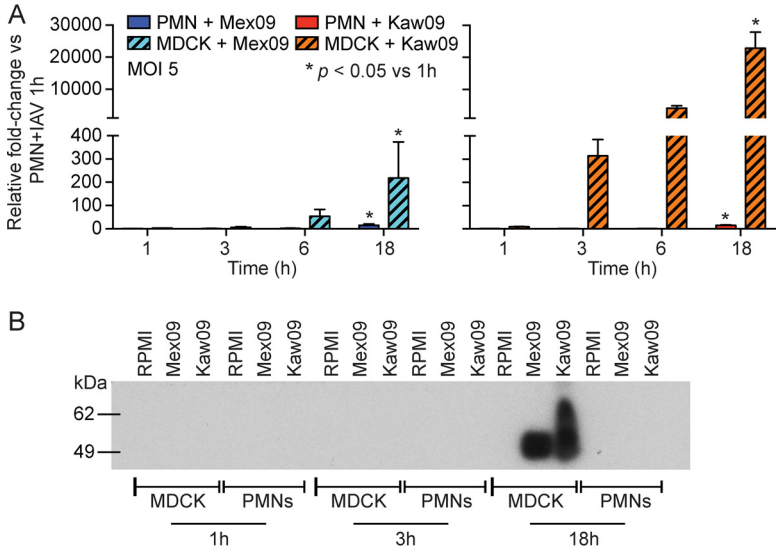

FIG 2 H1N1 IAV RNA synthesis and protein production in human neutrophils. (A) TaqMan real-time RT-PCR analysis of viral loads over time. Results are expressed as average relative fold changes in the IAV target matrix gene transcripts (*fluM*) relative to *GAPDH* transcripts in three blood donors. Statistical analyses were performed for each virus and each cell type. *, $P < 0.05$ versus the 1-h time point. (B) Immunoblot analysis of IAV HA in whole-cell lysates. The image shown is a representative of at least three experiments performed with neutrophils purified from three different donors. MDCK cells were used as a positive control for viral replication and protein production.

beling combined with fluorography versus detection by immunoblotting—explain these differences. A more recent study by Zhang et al. (32) suggests that there is a release of infectious IAV progeny from human neutrophils. In accordance with our current results, several other studies failed to provide compelling evidence that neutrophils produce infectious virus progeny, despite having the ability to amplify viral RNA (31, 33, 34).

IAV alters the neutrophil life span. IAV has been reported to decrease the neutrophil life span (35, 36). Therefore, we compared the abilities of seasonal and pandemic H1N1 IAV strains to alter neutrophil apoptosis and viability (Fig. 3). Neutrophils displayed features of early apoptosis (surface expression of phosphatidylserine) by 1 h of coculture with Mex09 or Kaw09 at an MOI of 1 (Fig. 3A). In contrast, neutrophils exposed to either IAV strain at an MOI of 10 or to heat-inactivated virus had significantly lower levels of surface-expressed phosphatidylserine than control neutrophils did 6 h after coculture (Fig. 3A). The molecular basis for this observation is unclear, since neutrophil viability in these assays was virtually identical for up to 6 h (Fig. 3B). Thus, the reduced levels of annexin V-fluorescein isothiocyanate (FITC) staining at high IAV MOIs at 6 h cannot be explained by cell loss. Compared to the viability of control untreated neutrophils, that of neutrophils cocultured with either IAV strain was significantly reduced at 18 h, but the decrease was relatively modest (e.g., 60.6% of neutrophils cultured with Kaw09 at an MOI of 1 were viable at 18 h, compared with 88.2% of control cells) (Fig. 3B). Greater than 50% of all neutrophils, including untreated control cells, were terminal deoxynucleotidyltransferase-mediated dUTP-biotin nick end labeling (TUNEL) positive by 18 h of culture (Fig. 3C), and the percentages of TUNEL-positive neutrophils were similar for Mex09 and Kaw09 (Fig. 3C). These findings suggest that any differences in neutrophil function imparted by Mex09 or Kaw09 are not due to a differential ability of these viruses to alter the neutrophil life span.

H1N1 upregulates expression of neutrophil transcripts encoding molecules involved in the host response to viruses. To gain insight into the molecular basis of differences in known disease phenotype between individuals infected with Mex09 or Kaw09, we evaluated global changes in human neutrophil gene expression during coculture with these IAV strains for up to 18 h (Fig. 4; Table S1). Compared to control

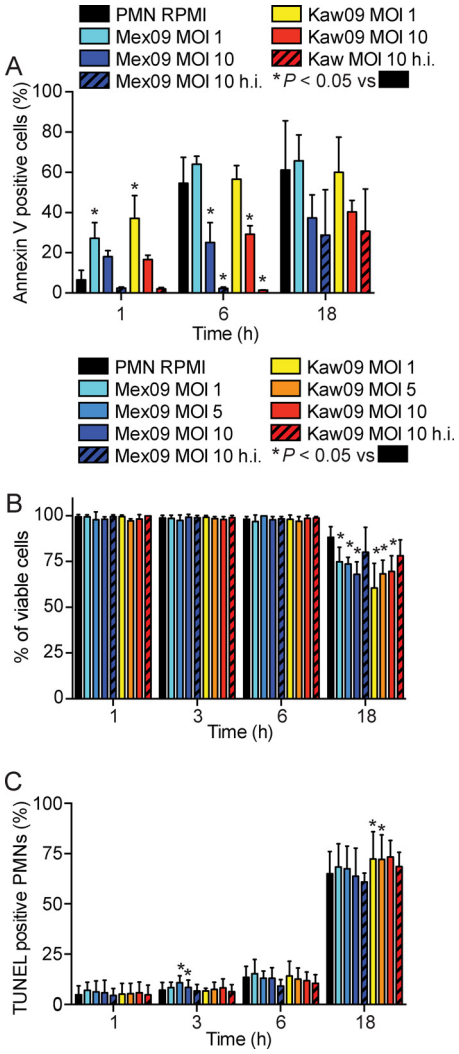

FIG 3 H1N1 IAV alters the neutrophil life span. Human neutrophils were incubated with Kaw09 or Mex09 influenza virus at an MOI of 1 to 10 or heat-inactivated (h.i.) virus as indicated. At selected time points, cell viability was assessed by annexin V-FITC-PI staining (A), trypan blue exclusion (B), or TUNEL assay (C). Results are presented as the means from at least three separate experiments. *, $P < 0.05$ versus control neutrophils (PMN RPMI) at the same time point.

cells, changes in neutrophil transcript levels were greatest at 6 and 18 h of coculture with IAV. Each of the viruses caused upregulation of transcripts encoding immune response molecules (Fig. 4; Table S1). In particular, there was upregulation of genes encoding virus pattern recognition receptors related to RIG-I-like receptors (RLRs), namely, *DDX58* (RIG-I) and *IFIH1* (MDA5). There was also increased expression of transcripts encoding upstream mediators of RLRs, such as *DHX58* (LPG2) and *DDX60*/*DDX60L* (Fig. 4; Fig. S2). Recognition of viral double-stranded RNA (dsRNA) by oligoadenylate synthetase (OAS) family molecules leads to activation of these host molecules and cleavage of viral RNA, which then is recognized by RLRs (37, 38). OAS family transcripts, namely, *OAS1*, *OAS2*, *OAS3*, and *OASL*, were upregulated in neutrophils 6 and 18 h after coculture with Mex09 or Kaw09 (Fig. 4). In addition, multiple genes known to be induced by interferon (IFN) were upregulated at these time points, including the gene encoding myxovirus resistance protein 1 (*MX1*), *IFI6*, *IFI35*, *IFI44*, *IFI44L*, genes encoding IFN-induced proteins with tetratricopeptide repeats (*IFIT1*, *IFIT2*, *IFIT3*, and *IFIT5*), and IFN-stimulated gene 15 (*ISG15*) (Fig. 4; Fig. S2). ISG15 plays a key role in the antiviral response either by its conjugation to target proteins (ISGylation) or as an unconjugated protein (39). *HERC5*, which encodes an E3 ligase that facilitates the

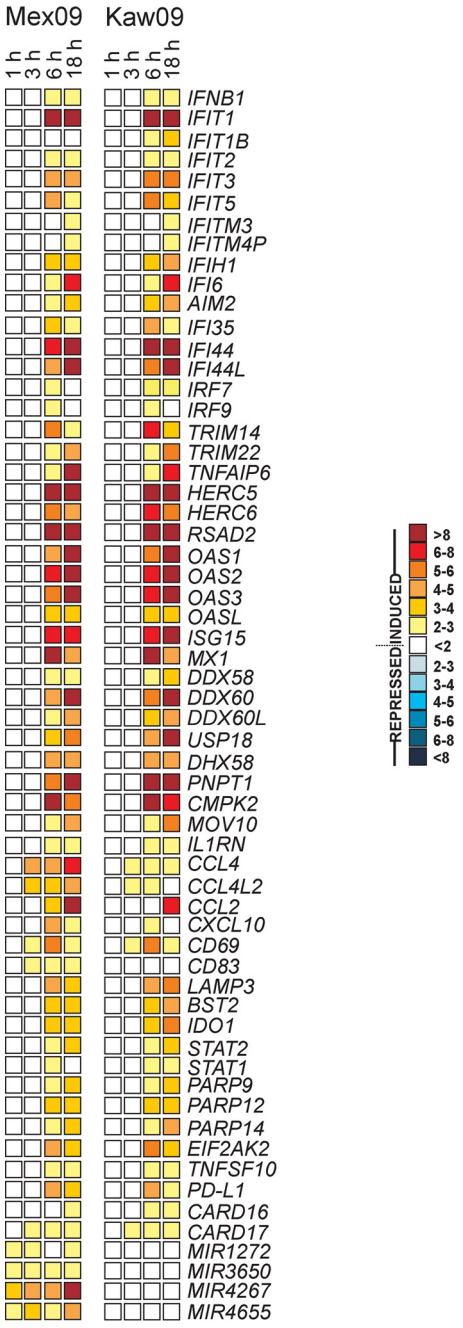

FIG 4 Immune response-related transcripts upregulated in neutrophils during coculture with IAV. Microarray results are presented as mean fold changes in three separate experiments (neutrophils from three separate individuals).

conjugation of ISG15 to target proteins, was upregulated 15- and 12-fold in neutrophils 6 h following culture with Kaw09 and Mex09, respectively (Fig. 4). Additionally, ISG15 directly targets the NS1 protein of IAV and inhibits virus replication (40, 41). Taken together, these results indicate that IAV elicits changes in neutrophil gene expression that are typical of a type I IFN response (Fig. 5). Indeed, treatment of neutrophils with ruxolitinib, a JAK1/JAK2 inhibitor (and thus an inhibitor of IFN signaling) blocked the ability of IAV to upregulate neutrophil genes crucial for antiviral responses, including *MX1*, *OAS1*, and *ISG15* (Fig. 6A; Table S2). However, ruxolitinib did not alter the amount of detectable viral transcripts in human neutrophils for up to 6 h after coculture with IAV (Fig. 6B).

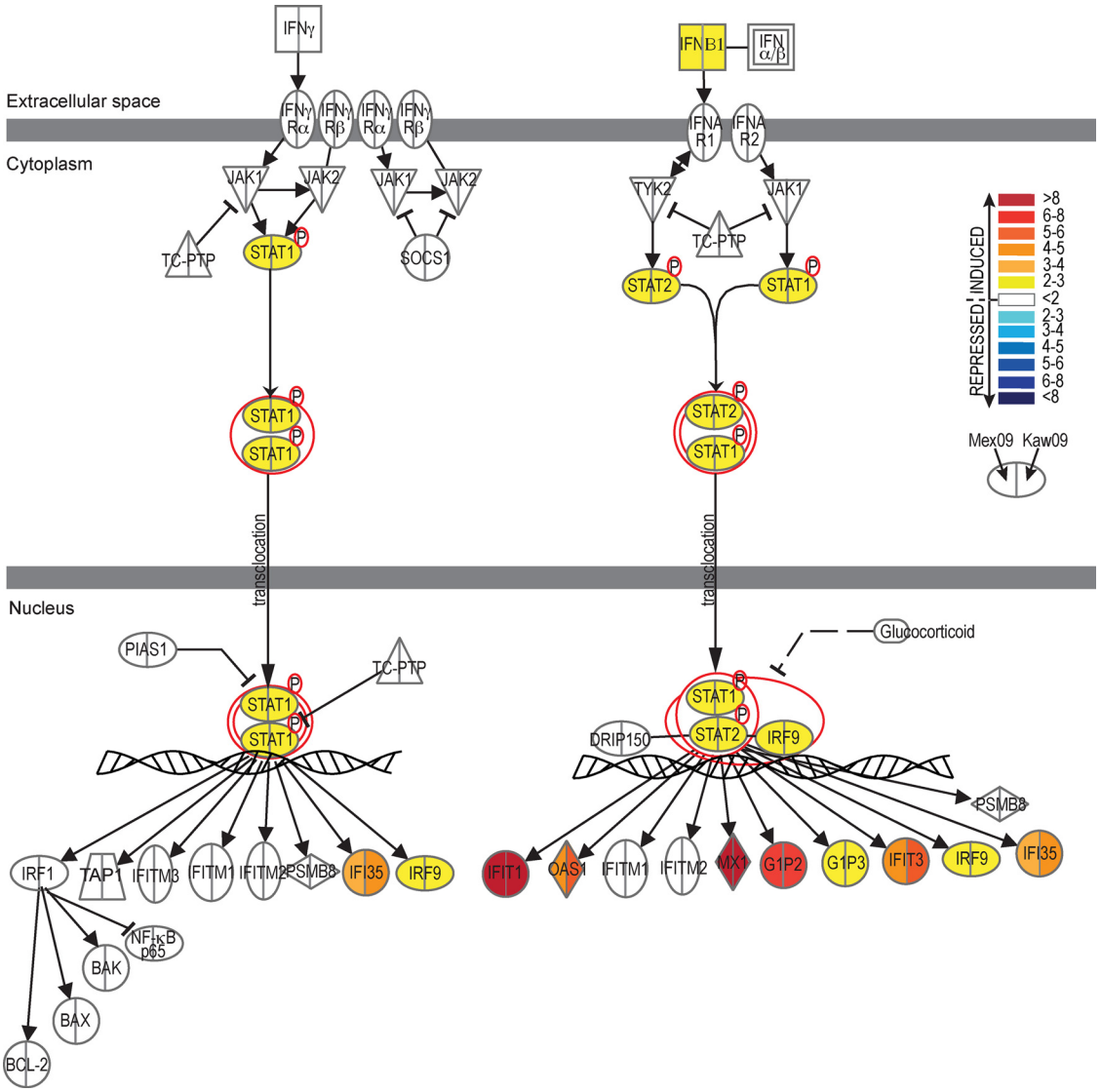

FIG 5 IAV upregulates genes involved in IFN signaling pathways. The networks/functional analyses were generated with IPA software (Qiagen). Fold changes in neutrophil transcript levels were determined by microarray analyses after coculture with Mex09 or Kaw09 (each at an MOI of 5) for 6 h. The key on the upper right indicates fold changes. The left half of each molecule represents neutrophils cultured with Mex09. The right half of the molecule indicates neutrophils cultured with Kaw09.

Although patterns of neutrophil gene expression were, in general, similar during coculture with pandemic and seasonal IAVs, a few differences were noted. For example, *MIR1272*, *MIR3650*, *MIR4267*, and *MIR4655*, microRNAs that are involved in the post-translational regulation of gene expression, were upregulated only in neutrophils cocultured with Mex09 (Fig. 4). Moreover, the upregulation of *CCL2*, *CCL4*, *CCL4L2*, and *CXCL10*, genes that encode chemokines secreted during IAV pneumonia (42), was greater in neutrophils cocultured with Mex09 than in those cocultured with Kaw09 (Fig. 4). Nonetheless, the observation that changes in the neutrophil transcriptome are similar following coculture with either pandemic or seasonal H1N1 virus seems to be at variance with published gene expression profiles in bronchoalveolar lavage fluid or bronchial or lung epithelial cells following exposure to these viruses (15, 42). Pandemic IAVs or those that cause more severe infections typically trigger high production of proinflammatory cytokines and chemokines (for example, interleukin-8 [IL-8], IL-6, MIP-1β, and MCP-1) that results in a massive influx of leukocytes, including neutrophils (13, 42–44). Apart from neutrophils playing a role in defense against influenza virus

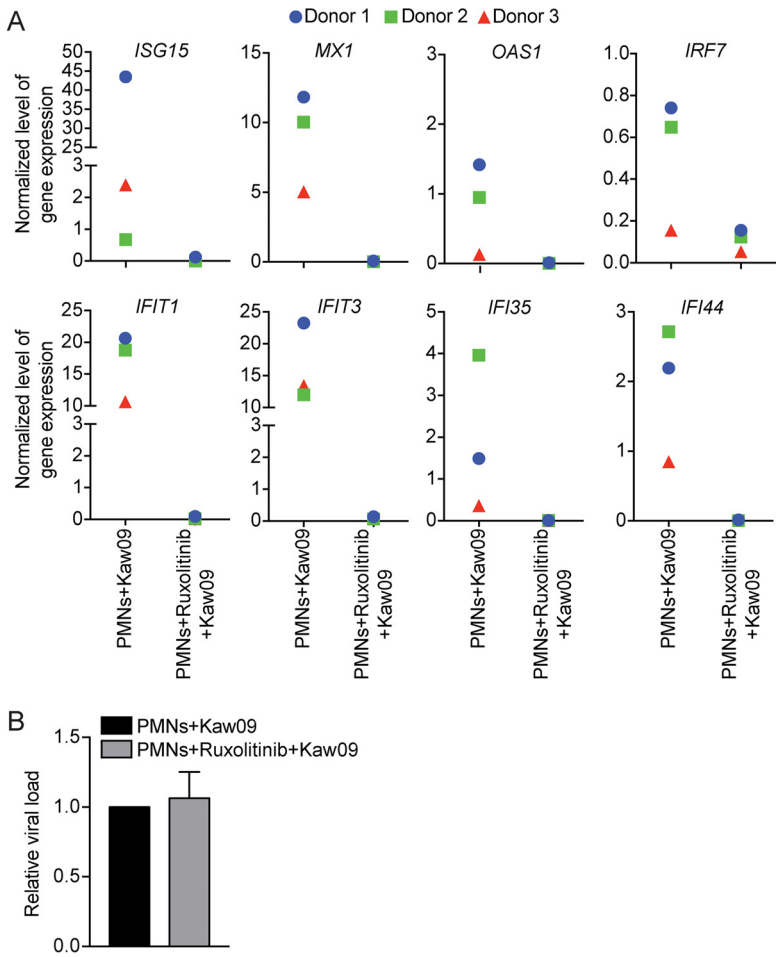

FIG 6 IAV-mediated changes in neutrophil transcripts are JAK/STAT dependent. Shown are the effects of a JAK1/JAK2 inhibitor on the levels of expression of selected neutrophil antiviral transcripts (A) and viral loads (B). (A) Neutrophils were pretreated with 20 µM ruxolitinib, and changes in gene expression were determined with a Human IFN and Receptor RT2 Profiler PCR Array (Qiagen). Gene expression levels were normalized against five housekeeping genes in the array panel. Results are presented as normalized gene expression from each neutrophil donor as indicated. (B) Results are expressed as the average relative fold change in the IAV target matrix gene transcript (*fluM*) relative to the control sample (neutrophils + Kaw09) and normalized against *GAPDH* for three blood donors.

infection (45), an increased influx of neutrophils into the lungs during respiratory tract infection and their subsequent lysis could also be deleterious to host tissue (46–50).

Genes encoding molecules known to promote apoptosis were upregulated in neutrophils cultured with Mex09 or Kaw09. Compared to control neutrophils, *EIF2AK2*, which encodes the IFN-induced dsRNA-activated protein kinase (PKR); *TNFSF10*; *PD-L1*; *CARD16*; and *CARD17* were upregulated in cells cultured with IAV (Fig. 4). In addition, the OAS and RNase L system is known to promote apoptosis in virus-infected cells as a host defense mechanism and several genes encoding OAS (*OAS1*, *OAS2*, and *OAS3*) were upregulated in neutrophils cultured with IAV (Fig. 4). Upregulation of these factors corresponds to data in Fig. 3B that show a slight but significant decrease in neutrophil viability at 18 h in the presence of active IAV compared to that of control cells (Fig. 3B).

H1N1 IAV primes neutrophils for enhanced function. We next tested whether the observed IAV-mediated changes in neutrophil gene expression, and notably those involved in the antiviral response, were reflected by changes in cell function. Phagocytosis of bacteria and fungi by neutrophils is normally followed by fusion of cytoplasmic granules with newly formed phagosomes. This process, known as degranulation, enriches microbe-containing phagosomes with antimicrobial peptides and proteins.

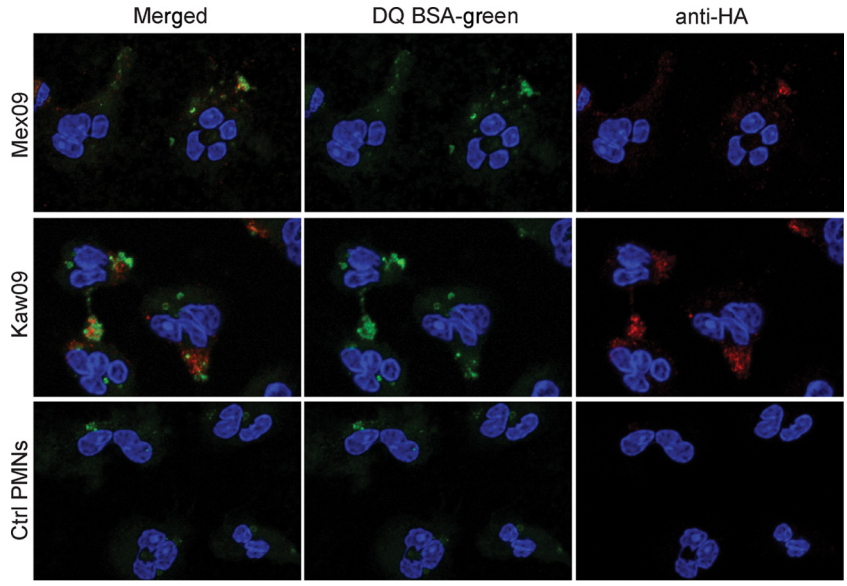

FIG 7 Colocalization of IAV and neutrophil protease activity. Neutrophils were incubated with Mex09 or Kaw09 at an MOI of 10 for 30 min. IAV was visualized with an anti-HA antibody (red), protease activity was detected with DQ Green BSA (green), and neutrophil nuclei were stained with DAPI (blue). Images are representative of at least three experiments performed with neutrophils obtained from three different blood donors.

Although any ingested IAV was located within a membrane-bound vacuole (Fig. 1C) and protease activity was colocalized with IAV (Fig. 7), there was little or no colocalization of IAV with CD35 (a receptor present in the membranes of secretory vesicles) or with CD63 (a component of the membranes of azurophilic granules) (Fig. 8; Fig. S3). Thus, fusion of cytoplasmic granules with IAV-containing vacuoles failed to occur under our assay conditions. Additionally, neither Mex09 nor Kaw09 caused an immediate increase in the surface expression of CD11b, a phenomenon characteristic of secretory vesicle or granule exocytosis (Fig. 9A). Instead, both viruses inhibited the surface expression of CD11b when cocultured with neutrophils for 60 min (Fig. 9B). Nonetheless, this inhibition did not alter the ability of a secondary stimulus, such as *N*-formylmethionyl-leucyl-phenylalanine (fMLF), to activate neutrophils (Fig. 9B). Collectively, these findings are in agreement with previous studies by Abramson et al., who reported the ability of IAV to inhibit the fusion of azurophilic granules with phagosomes and to block endocytosis (16, 30).

Neither Mex09 nor Kaw09 alone caused production of reactive oxygen species (ROS) by human neutrophils (Fig. 9C). However, preincubation with Kaw09—but not Mex09—enhanced the production of neutrophil ROS following the phagocytosis of opsonized zymosan (OPZ) (Fig. 9D). More notably, preincubation with Kaw09 significantly increased the ability of human neutrophils to kill *S. aureus* (e.g., the survival of *S. aureus* was 54.7% $\pm$ 7.2% in neutrophils preincubated with Kaw09 and 74.1% $\pm$ 12.3% in control neutrophils [$P = 0.027$]) (Fig. 9E). *S. aureus* survival was also decreased following culture with neutrophils preincubated with Mex09, but the difference was not significant. The ability of IAV to enhance the killing of *S. aureus* by neutrophils was not linked to increased phagocytosis, since the uptake of *S. aureus* by neutrophils was not altered by preincubation with IAV (Fig. 9F). Collectively, these findings seem to be at variance with previous studies that reported the ability of IAV to depress neutrophil functions, including inhibition of ROS and bactericidal activity (19). Whether the IAV-mediated priming for enhanced ROS production by neutrophils is a direct reflection of bactericidal activity remains to be determined. Our data demonstrate that neither Mex09 nor Kaw09 activated polymorphonuclear leukocytes (PMNs or neutrophils) directly. Rather, the seasonal IAV strain used here—Kaw09—primed neutrophils for

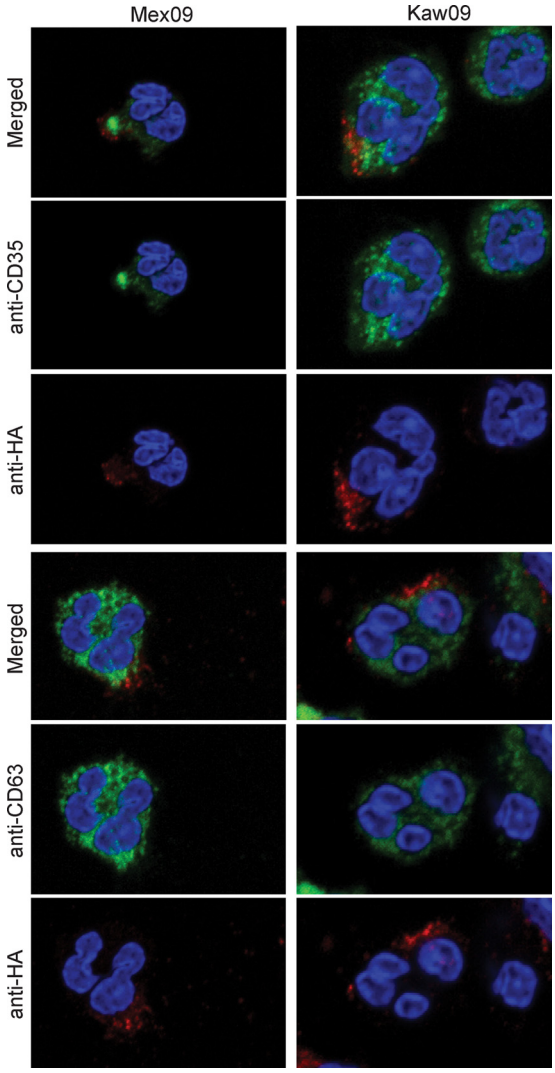

FIG 8 Proteins from azurophilic granules and secretory vesicles fail to colocalize with IAV. Neutrophils were incubated with Mex09 or Kaw09 for 30 min, and colocalization of CD35 (a marker for secretory vesicles) or CD63 (a marker for azurophilic granules) was evaluated by immunofluorescence microscopy. CD35 or CD63 was detected with an antibody specific for each protein (green) as indicated. IAV was visualized with an anti-HA antibody (red), and DAPI was used to stain the nucleus (blue). Images are representative of at least three experiments performed with neutrophils obtained from three different blood donors.

enhanced bactericidal activity. In contrast to our findings, previous studies reported that IAV inhibits neutrophil function and this phenomenon has long been considered an explanation, in part, for host susceptibility to secondary bacterial infections in individuals with primary IAV pneumonia. It is possible that the differences between our study and previous studies can be explained by differences between the IAV strains used. Indeed, Abramson et al. demonstrated that some IAV strains depress neutrophil functions whereas others fail to do so (16, 30). Moreover, a recent study by Robinson et al. reported that IAV impairs the Th17 pathway but not neutrophil function, and this process, in turn, reduces the host defense against *S. aureus* (51). Our study was designed to investigate the ability of IAV to alter the function of human neutrophils apart from the complexity of stimuli present during infection *in vivo*. Although this approach answers some basic questions related to direct interactions between IAV and neutrophils, it is limited by controlled experimental conditions *in vitro* and does not fully recapitulate the *in vivo* infection process. More work is needed to better under-

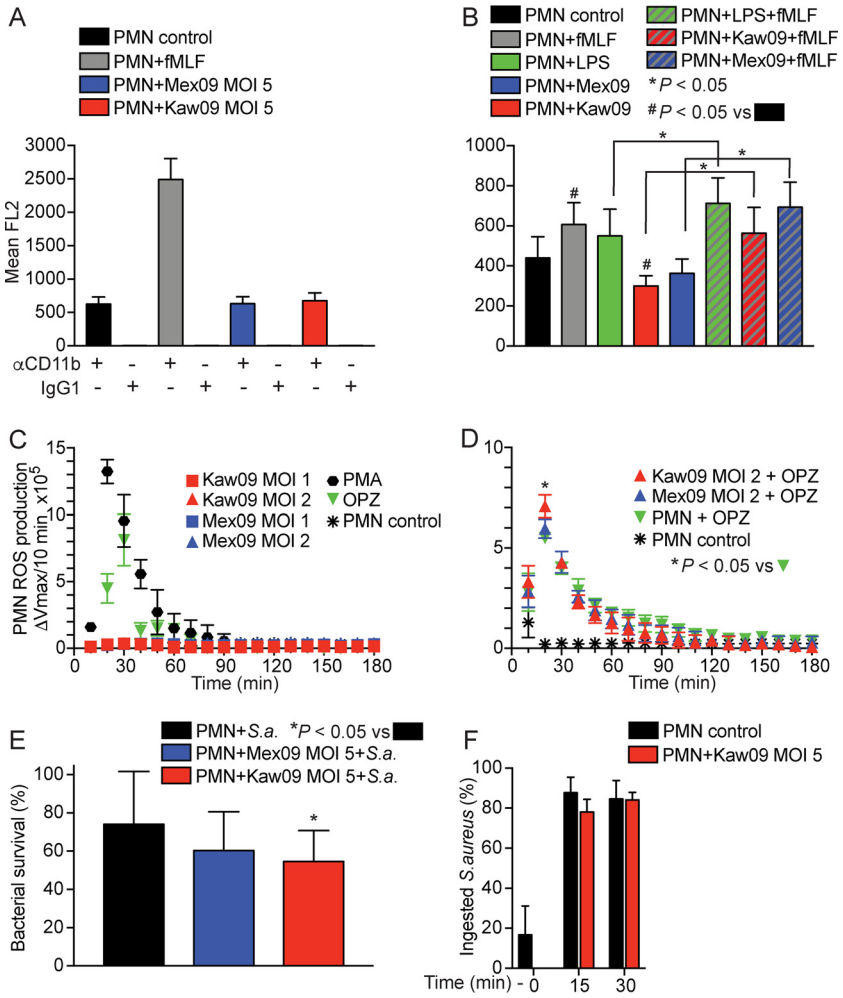

FIG 9 IAV alters neutrophil bactericidal activity. (A) Surface expression of CD11b was measured by flow cytometry after a 15-min coculture with IAV or 1 µM fMLF. The presence (+) or absence (−) of IgG1 (isotype control antibody) or an antibody specific for CD11b (αCD11b) is indicated on the *x* axis. (B) Surface expression of CD11b was measured after 60 min of neutrophil coculture with lipopolysaccharide (LPS), 1 µM fMLF, or IAV alone, as indicated. Alternatively, neutrophils were cocultured with LPS or IAV (MOI of 5) for 60 min and stimulated for 10 min with 1 µM fMLF as indicated and surface expression of CD11b was measured by flow cytometry. (C) Neutrophil ROS were measured following coculture with PMA (positive control), OPZ (positive control), or IAV. (D) Production of neutrophil ROS was measured after stimulation of cells with OPZ following a 60-min preincubation with IAV as indicated. (E) The ability of neutrophils to kill *S. aureus* (*S.a.*) strain USA300 (1:1 bacterium-to-neutrophil ratio) was increased following coculture with IAV. (F) Uptake of *S. aureus* by neutrophils was evaluated by fluorescence microscopy. The assay was performed with a bacterium-to-neutrophil ratio of 1:1, and samples were preincubated with Kaw09 at an MOI of 5 for 3 h, as indicated. Data are the means from at least three experiments (three blood donors) and were analyzed by RM one-way ANOVA and Dunnett's posttest (for panels A, C, D, and E), Bonferroni's posttest (panel B), or a paired two-tailed *t* test (panel F).

stand whether a direct interaction of IAV with neutrophils contributes significantly to the pathogenesis of bacterial infections with antecedent IAV infection.

MATERIALS AND METHODS

Ethics statement. Venous blood was obtained from healthy human volunteers. The Institutional Review Board for Human Persons, National Institute of Allergy and Infectious Diseases, National Institutes of Health, approved these studies (protocol 01-I-N055). All study participants provided written consent prior to enrollment.

Virus propagation and purification. A/Mexico/4108/2009 (H1N1) (Mex09) represents the 2009 pandemic IAV strain and was isolated from a clinical specimen (kindly provided by the Centers for Disease Control and Prevention Influenza Branch) obtained from a 4-year-old boy from Mexico who was mildly ill (13). A/Kawasaki/UTK-4/2009 (H1N1) (Kaw09) was isolated from a human and represents a recent seasonal IAV strain (14). Viruses were propagated in MDCK cell culture as previously described

(13). To purify and concentrate the virus stock, cell culture supernatant was clarified by centrifugation at 1,700 × *g* for 15 min at 4°C, overlaid onto 20% sucrose in Dulbecco's phosphate-buffered saline (DPBS; Sigma-Aldrich, St. Louis, MO), and centrifuged at 110,000 × *g* for 2.5 h at 4°C. The resulting pellet was suspended in RPMI 1640 medium (Invitrogen/Life Technologies, Inc., Grand Island, NY) buffered with 10 mM HEPES (RPMI/H; Mediatech, Manassas, VA). The viral stock was stored at −80°C until used. The virus titer was determined by plaque-forming assay using MDCK cells cultured in six-well plates with a medium-viscosity carboxymethyl cellulose sodium salt (Sigma-Aldrich, St. Louis, MO) overlay (52, 53). Heat inactivation of the virus was achieved by 10 min of incubation at 100°C and verified by plaque-forming assay. The virus strains used in this study are biosafety level 2 viruses. All infectious samples were handled in accordance with a human pathogen registration document approved by the Institutional Biosafety Committee at Rocky Mountain Laboratories, Division of Intramural Research, National Institute of Allergy and Infectious Diseases, National Institutes of Health.

Neutrophil isolation. Human PMNs were isolated from fresh heparinized venous blood by standard dextran sedimentation coupled with Hypaque-Ficoll gradient centrifugation as previously described (54). The viability and purity of all neutrophil preparations were assessed by flow cytometry. Neutrophil preparations typically yield 98 to 99% PMNs (of which ~95 to 98% were neutrophils and ~2 to 5% were eosinophils), and viability was ≥99% as assessed by uptake of propidium iodide (PI).

Neutrophil viability. Neutrophil apoptosis and viability were examined by staining with annexin V-FITC-PI, TUNEL, and a trypan blue exclusion assay. Assays were performed in 24- or 96-well round-bottom tissue culture plates precoated with 20% normal human serum (NHS). Neutrophils were cultured with IAV at MOIs ranging from 0 to 10 at 37°C with 5% CO_2 and 90% humidity for up to 18 h. At designated time points, samples were processed in accordance with the manufacturer's protocol for each assay. Early apoptosis was evaluated on the basis of surface staining with annexin V-FITC (for exposure of the phospholipid phosphatidylserine) and uptake of PI (FITC Annexin V Apoptosis Detection Kit II; BD Pharmingen, San Diego, CA). DNA fragmentation was assessed with a TUNEL assay (APO-BRDU kit; BD Biosciences, San Diego, CA) as described elsewhere (54). To comply with institutional biosafety requirements, all samples were fixed with ice-cold 4% paraformaldehyde prior to analysis on a FACSCalibur flow cytometer (BD Biosciences). Ten thousand events were collected for each sample. Additionally, neutrophil viability was assessed in a trypan blue exclusion assay. Briefly, at the desired time point, neutrophils were collected from the cell culture plate, transferred into 1.5-ml tubes, and incubated with a trypan blue solution (2 mg/ml trypan blue [JT Baker Chemical Co., Phillipsburg, NJ], 0.02 M sodium citrate, 0.15 M NaCl, pH 4.4). Cells were enumerated with a hemocytometer and a light microscope, and the percentage of viable cells was calculated by using the following equation: (number of cells that exclude trypan blue/total number of cells) × 100.

Immunofluorescence microscopy. Neutrophils (3×10^5) were added to 24-well culture plates containing acid-washed coverslips coated with 100% pooled NHS. H1N1 Mex09 or Kaw09 was added at an MOI of 10 to experimental samples, and an equivalent volume of RPMI/H was added to control samples. Samples were centrifuged at 450 × *g* for 6 min to synchronize phagocytosis. DQ Green BSA (50 µg/ml; Molecular Probes, Eugene, OR) was added to the group of samples to track protease activity. Samples were incubated for up to 1 h at 37°C. At the desired time point, supernatant was aspirated and neutrophils were washed once with DPBS (Sigma-Aldrich, St. Louis, MO). Cells were fixed with 4% paraformaldehyde (Electron Microscopy Sciences, Hatfield, PA) in DPBS. Consequently, cells were permeabilized with 0.2% Triton X-100 (USB, Cleveland, OH) in DPBS for 15 min at ambient temperature. Cells were washed twice with DPBS and blocked with Stain Buffer (FBS) (BD Biosciences, San Jose, CA) for 10 min. Samples were incubated with selected antibodies in Stain Buffer (FBS) for 1 h at ambient temperature with gentle agitation. Prior to incubation with secondary antibodies (where appropriate), cells were washed three times with DPBS. The antibodies used for cell labeling were FITC-labeled mouse anti-human CD63 (40 µl/sample) and anti-human CD35 (60 µl/sample) (BD Pharmingen), Alexa Fluor 488-conjugated phalloidin (1 U/sample) (Molecular Probes/Thermo Fisher Scientific, Inc., Eugene, OR), and a mouse anti-IAV H1N1 hemagglutinin (HA) monoclonal antibody (final concentration, 4 to 10 µg/ml) (Thermo Fisher Scientific, Inc., Rockford, IL) in combination with an Alexa Fluor 594-conjugated goat anti-mouse IgG (H+L) secondary antibody (Molecular Probes/Thermo Fisher Scientific, Inc., Eugene, Eugene, OR) at a final concentration of 0.1 µg/ml. To evaluate the uptake of virus particles by neutrophils or MDCK cells, cells were first incubated with a rabbit anti-IAV H1N1 HA polyclonal antibody (Thermo Fisher Scientific, Inc., Rockford, IL) at a final concentration of 10 µg/ml. After being washed, samples were incubated with an Alexa Fluor 488-conjugated goat anti-rabbit IgG (H+L) cross-adsorbed secondary antibody (final concentration, 0.1 µg/ml). This first procedure stains all surface-bound (extracellular) IAV. Subsequently, neutrophils were permeabilized as described above and stained with a sequential combination of a rabbit anti-IAV H1N1 HA polyclonal antibody (primary antibody) and an Alexa Fluor 594-conjugated goat anti-rabbit IgG (H+L) cross-adsorbed secondary antibody (final concentration, 0.1 µg/ml). This procedure stains surface-bound and ingested (extracellular and intracellular) IAV. Coverslips were mounted with Fluoromount G containing 4′,6-diamidino-2-phenylindole (DAPI; Electron Microscopy Sciences, Hatfield, PA). Samples were imaged on a Carl Zeiss, Inc., LSM710 confocal laser-scanning microscope equipped with ZEN software version 8.1.10 (Carl Zeiss, Inc., Thornwood, NY). Image contrast and brightness were adjusted in ZEN software or by using Adobe Photoshop CS5.1 (Adobe, San Jose, CA). The percentage of neutrophils with intracellular IAV was determined with the following equation: $PMN_{intracellular\ IAV}/PMN_{total} \times 100$. At least 50 cells in five separate fields of view per sample were used to calculate the uptake of IAV.

Transmission electron microscopy (TEM). Human neutrophils were seeded onto NHS-coated Thermanox coverslips and incubated with IAV at an MOI of 20 for up to 3 h in 24-well cell culture plates

at 37°C. Samples were then washed once with DPBS and fixed for 30 min with 2.5% glutaraldehyde in 0.1 M sodium cacodylate buffer, pH 7.4. All subsequent processing was carried out in a PELCO BioWave Pro laboratory microwave (Ted Pella, Inc., Redding, CA.). Neutrophils were postfixed with 1% osmium tetroxide reduced with 0.8% potassium ferrocyanide in 0.1 M sodium cacodylate buffer, treated with 1% tannic acid, and stained en bloc with uranyl acid replacement stain. The cells were dehydrated in a gradient ethanol series and infiltrated with Embed 812 resin. The resin blocks were polymerized overnight in an oven at 65°C. Thin sections were cut with a Leica UC6 ultramicrotome (Leica Microsystems, Inc., Vienna, Austria) and examined with an 80-kV Hitachi 7500 transmission electron microscope (Hitachi High Technology in America, Schaumburg, IL). Images were captured with a bottom mount AMT camera system (Advanced Microscopy Techniques Corp., Woburn, MA).

Microarray experiments. Twenty-four-well culture plates were coated with 20% pooled NHS for at least 1 h at 37°C. Plates were washed twice with DPBS and kept on ice until used. A total of 5×10^6 neutrophils were added to each well, and the cells were infected with IAV at an MOI of 5. For control samples, an equivalent volume of RPMI/H was added instead of virus. Neutrophils from three different human blood donors were used for microarray experiments. Samples were incubated for up to 18 h at 37°C with 5% CO_2. At selected time points (1, 3, 6, and 18 h), samples were centrifuged at 500 $\times$ *g* for 8 min at 4°C. Supernatant was aspirated, and cells were treated with TRIzol (Ambion/Life Technologies, Carlsbad, CA) for 5 min and frozen at −80°C until samples were collected all time points. Total RNA was purified with a Direct-zol RNA MiniPrep kit in accordance with the manufacturer's protocol (Zymo Research Corp., Irvine, CA). The remaining DNA was removed with Turbo DNase (Ambion/Applied Biosystems, Austin, TX), and samples were repurified with an RNeasy minikit (Qiagen, Hilden, Germany). The quantity and quality of isolated RNA were assessed with a 2100 Bioanalyzer (Agilent Technologies, Santa Clara, CA). RNA amplification and labeling were carried out with a GeneChip WT PLUS Reagent kit (Affymetrix/Thermo Fisher, Santa Clara, CA) in accordance with the manufacturer's protocol. Labeled samples were hybridized to GeneChip Human Gene 2.0 ST Arrays. GeneChips were scanned with the Affymetrix GeneChip 3000 7G Plus scanner in accordance with a standard GeneChip protocol, and the image files were converted to .Cel files with Expression Console (v1.4). Quality analysis was performed in accordance with the white paper *Quality Assessment of Exon and Gene Arrays* (Affymetrix revision 11). All .Cel files, representing individual samples, were normalized by the RMA method within Expression Console to produce chip (.chp) files. A report was generated from the .chp files (along with selected raw data) summarizing various quality and statistical aspects of the chips. One sample (the neutrophil control at 3 h, one donor) was indicated as a quality outlier and excluded from the analysis. Except for the neutrophil control at 3 h, expression microarray data are presented as the mean fold change of three separate donors. Statistical analyses were performed by analysis of variance (ANOVA) and multiple-test correction by using the false-discovery rate (FDR; significance at a level of 0.05 [55]) (Partek Genomics Suite software, v6.5 6091110 [Partek, Inc., St. Louis, MO]). These data were combined with fold change values by using custom Excel templates to generate final gene lists for each comparison (Table S1). Microarray data were analyzed additionally with Ingenuity Pathway Analysis (IPA) software (Qiagen, Redwood City, CA) to identify functional groups, gene networks, and canonical pathways. Figures were created with Adobe Illustrator CC2015.3 software.

TaqMan real-time RT-PCR. RNA samples used in the microarray experiment were also analyzed by TaqMan real-time RT-PCR to assess viral loads. Alternatively, to compare viral replication in neutrophils with that in MDCK cells, total RNA was isolated from infected MDCK cells (or uninfected samples, which served as a negative control) as described above. Twenty-five nanograms of total purified RNA was subjected to one-step qRT-PCR with the AgPath-ID one-Step RT-PCR kit and an ABI 7500 thermocycler (Ambion/Applied Biosystems, Foster City, CA). The relative quantification of viral RNA was done by measuring the change in the expression level of the target matrix gene transcripts (*fluM* [56]) relative to the *GAPDH* transcripts (GAPDH TaqMan Gene Expression Assays; Applied Biosystems, Foster City, CA) in accordance with the manufacturer's protocol (Applied Biosystems relative quantification manual). Data are expressed as the mean fold differences between the transcript levels at 3, 6, and 18 h and the transcript level at 1 h for each virus.

PCR arrays. Neutrophils were preincubated with 20 μM ruxolitinib (Selleck Chemicals, Houston, TX) or an equal volume of RPMI/H for 2 h at 37°C with 5% CO_2. Subsequently, Kaw09 was added at an MOI of 5 and samples were incubated for an additional 6 h. At the time point indicated, RNA was isolated as described in the section on microarray experiments. Five hundred nanograms of purified RNA was used to synthesized cDNA with an RT^2 First Strand kit (Qiagen). Expression levels of genes encoding human IFNs and receptors were detected with the Human IFNs and Receptors RT^2 Profiler PCR Array platform in combination with RT^2 Sybr green ROX qPCR Mastermix (Qiagen) in accordance with the manufacturer's instructions. Samples were amplified with an ABI 7500 real-time PCR system (Applied Biosystems). Data analysis was performed with a template downloaded from the Qiagen genes and pathways data analysis center overview page, and gene expression levels were normalized against all five housekeeping genes.

Immunoblotting. Neutrophils were incubated with buffer alone (control), Mex09, or Kaw09 at an MOI of 5 for up to 18 h at 37°C with 5% CO_2. At designated time points, cells were pelleted by centrifugation at 450 $\times$ *g* for 7 min at ambient temperature. Neutrophils were suspended in lysis buffer (50 mM Tris [pH 7.5], 280 mM NaCl, 1% Triton X-100, 0.2 mM EDTA, 2 mM EGTA, 10% glycerol, 1 mM dithiothreitol, 0.1 mM sodium vanadate) containing a protease inhibitor cocktail (cOmplete ULTRA Tablets, Mini, *EASYpack* Protease Inhibitor Cocktail; Roche, Indianapolis, IN) (57). IAV-infected MDCK cells were used as a positive control for viral protein production. Protein was quantitated with a bicinchoninic acid protein assay (Pierce Protein Research Products/Thermo Fisher Scientific, Rockford, IL), and 10 µg of protein was separated by 12.5% SDS-PAGE (Criterion; Bio-Rad, Hercules, CA). Proteins were

transferred to polyvinylidene difluoride membranes with the iBlot transfer system (Invitrogen/Thermo Fisher Scientific, Waltham, MA), and membranes were blocked for 1 h at ambient temperature in 5% dry milk powder (Research Products International, Mt. Prospect, IL) in PBS containing 0.05% Tween 20. Influenza virus HA was detected with a rabbit anti-IAV H1N1 HA polyclonal antibody. Membranes were incubated with a primary antibody (0.5 µg/ml) in blocking buffer overnight at 4°C. The following day, membranes were washed three times with wash buffer (250 mM NaCl, 10 mM HEPES, 0.2% Tween 20) and incubated for 1.5 h with a secondary antibody conjugated with horseradish peroxidase (HRP) (polyclonal goat anti-rabbit immunoglobulins/HRP; Dako/Agilent, Santa Clara, CA). The antibody-protein complex was visualized with Pierce ECL Plus Western blotting substrate (Pierce Biotechnology, Rockford, IL) and X-ray film (Phenix Research Products, Chandler, NC).

Neutrophil function assays. To determine changes in the surface expression of CD11b caused by IAV, neutrophils were incubated with IAV at an MOI of 5 or with 1 µM fMLF for 15 min at 37°C. Cells were washed and stained with a phycoerythrin (PE)-conjugated anti-human CD11b antibody or a PE-conjugated mouse isotype IgG1 control (58). Samples were fixed with 4% paraformaldehyde in DPBS, washed, and analyzed by flow cytometry. To evaluate the ability of IAV to prime human neutrophils, cells were preincubated with IAV at an MOI of 5 for 60 min at 37°C and stimulated with 1 µM fMLF for 10 min.

Production of neutrophil ROS was determined by oxidation of 2,7-dichlorodihydrofluorescein diacetate (DCF; Sigma-Aldrich, St. Louis, MO) as described previously (54) but with modifications. Black, flat-bottom 96-well culture plates were coated with 20% NHS for 1 h and washed twice with DPBS. Human neutrophils (10^7/ml) were preloaded with 25 µM DCF (Sigma-Aldrich) in the dark for 20 min at ambient temperature. Zymosan A (MP Biomedicals, Solon, OH) was opsonized with 50% NHS for 30 min at 37°C, washed twice with DPBS, and resuspended in RPMI/H (2.5×10^8 particles/ml). For each assay, 10^6 neutrophils (preloaded with DCF) were stimulated with IAV (MOI of 1 to 2), OPZ (~5 particles per neutrophil), or phorbol 12-myristate 13-acetate (PMA; 1 µg/ml; Sigma-Aldrich, St. Louis, MO) in a final volume of 200 µl. For assays in which neutrophils where primed with IAV, OPZ was added 60 min after the incubation of IAV alone. Neutrophil activation was synchronized by centrifugation at 500 $\times$ *g* for 7 min at 4°C. An optical adhesive cover (Applied Biosystems, Foster City, CA) was placed over the assay plate, and ROS production was monitored by measuring DCF fluorescence (excitation wavelength, 485 nm; emission wavelength, 538 nm) for 3 h at 37°C with a SpectraMax Gemini XPS plate reader (Molecular Devices, Sunnyvale, CA). Data are presented as the mean V_{max} at 10-min intervals under each assay condition. Data were analyzed by repeated-measures (RM) one-way ANOVA and Dunnett's posttest to correct for multiple comparisons.

S. aureus strain LAC, a USA300 isolate representative of the USA300 epidemic clone, from a frozen stock was cultured overnight in Trypticase soy broth (Difco, Detroit, MI). Overnight cultures were inoculated into fresh medium and cultured to the mid-logarithmic phase of growth (optical density at 600 nm of 0.75). Bacteria were collected by centrifugation, opsonized in 50% NHS for 30 min at 37°C, washed twice with DPBS, and resuspended in RPMI/H at a final concentration of 10^6 CFU/ml. Human neutrophils (10^5 CFU/ml) were incubated with IAV (MOI of 5) in 96-well flat-bottom plates (precoated with 20% NHS) for 3 h at 37°C. Bacteria were then added to assay wells (200-μl final volume) at a 1:1 bacterium-to-neutrophil ratio, and samples were incubated for an additional 1 h. At the desired endpoint, neutrophils were lysed with 0.1% saponin for 15 min on ice. Samples from each assay well were diluted and plated on Trypticase soy agar (Difco). The following day, bacterial CFU were enumerated and percent bacterial survival was calculated with the following equation: $CFU_{+PMN\ 1\ h}/CFU_{+PMN\ 0\ min} \times 100\%$.

To determine whether IAV altered the phagocytosis of *S. aureus*, human neutrophils (3×10^5) were combined with Kaw09 in 24-well tissue culture plates as described above for the bactericidal activity assay. In addition, wells contained acid-washed coverslips that had been precoated with 100% pooled NHS. Prior to the addition of bacteria, samples were chilled on ice for 10 min. Opsonized bacteria were stained with FITC (7.5 μg/ml) for 15 min at room temperature in the dark and washed twice with DPBS. Bacteria were then added to assay wells (500-μl final volume) at a 1:1 bacterium-to-neutrophil ratio, and samples were centrifuged at 450 $\times$ *g* for 7 min to synchronize phagocytosis. Plates were then incubated at 37°C for 0, 15, or 30 min. At the desired time points, supernatant was aspirated and neutrophils were washed once with DPBS. Cells were fixed with 4% paraformaldehyde in DPBS, and extracellular bacteria were stained with a rabbit anti-*S. aureus* polyclonal antibody (59) in combination with a goat anti-rabbit antibody conjugated with Alexa Fluor 594 (Molecular Probes, Life Technologies, Inc.). Coverslips were mounted with Fluoromount G containing DAPI, and the percentage of ingested bacteria was calculated for 50 neutrophils per blood donor (three donors total).

Statistical analyses. Data, except those from microarray experiments, were analyzed by RM one-way ANOVA and Dunnett's or Bonferroni's (for selected pair comparisons) posttest to correct for multiple comparisons or a paired *t* test, as indicated (Prism 7.0; GraphPad, San Diego, CA).

Accession number(s). All microarray data are MIAME (minimum information about a microarray experiment) compliant, and a complete set of microarray data has been posted online at http://www.ncbi.nlm.nih.gov/projects/geo/ under series number GSE100865.

SUPPLEMENTAL MATERIAL

Supplemental material for this article may be found at https://doi.org/10.1128/mSphereDirect.00567-17.

FIG S1, TIF file, 0.4 MB.

FIG S2, TIF file, 2.9 MB.

FIG S3, JPG file, 2.5 MB.
TABLE S1, XLSX file, 0.05 MB.
TABLE S2, PDF file, 0.1 MB.

ACKNOWLEDGMENT

This work was supported by the Intramural Research Program of the National Institute of Allergy and Infectious Diseases, National Institutes of Health.

REFERENCES

1. Rolfes MA, Foppa IM, Garg S, Flannery B, Brammer L, Singleton JA, Burns E, Jernigan D, Reed C, Olsen SJ, Bresee J. 2016. Estimated influenza illnesses, medical visits, hospitalizations, and deaths averted by vaccination in the United States. Centers for Disease Control and Prevention, Atlanta, GA. https://www.cdc.gov/flu/about/disease/2015-16.htm. Accessed 15 July 2017.
2. Morens DM, Taubenberger JK, Fauci AS. 2008. Predominant role of bacterial pneumonia as a cause of death in pandemic influenza: implications for pandemic influenza preparedness. J Infect Dis 198:962–970. https://doi.org/10.1086/591708.
3. Hers JFP, Masurel N, Mulder J. 1958. Bacteriology and histopathology of the respiratory tract and lungs in fatal Asian influenza. Lancet ii: 1141–1143. https://doi.org/10.1016/S0140-6736(58)92404-8.
4. Centers for Disease Control and Prevention. 2009. Bacterial coinfections in lung tissue specimens from fatal cases of 2009 pandemic influenza A (H1N1)—United States, May-August 2009. MMWR Morb Mortal Wkly Rep 58:1071–1074.
5. Finelli L, Fiore A, Dhara R, Brammer L, Shay DK, Kamimoto L, Fry A, Hageman J, Gorwitz R, Bresee J, Uyeki T. 2008. Influenza-associated pediatric mortality in the United States: increase of *Staphylococcus aureus* coinfection. Pediatrics 122:805–811. https://doi.org/10.1542/peds.2008-1336.
6. Christman MC, Kedwaii A, Xu J, Donis RO, Lu G. 2011. Pandemic (H1N1) 2009 virus revisited: an evolutionary retrospective. Infect Genet Evol 11:803–811. https://doi.org/10.1016/j.meegid.2011.02.021.
7. Virus Investigation Team (Team NS-OIAVI), Dawood FS, Jain S, Finelli L, Shaw MW, Lindstrom S, Garten RJ, Gubareva LV, Xu X, Bridges CB, Uyeki TM. 2009. Emergence of a novel swine-origin influenza A (H1N1) virus in humans. N Engl J Med 360:2605–2615. https://doi.org/10.1056/NEJMoa0903810.
8. Rice TW, Rubinson L, Uyeki TM, Vaughn FL, John BB, Miller RRI, Higgs E, Randolph AG, Smoot BE, Thompson BT; NHLBI ARDS Network. 2012. Critical illness from 2009 pandemic influenza A virus and bacterial coinfection in the United States. Crit Care Med 40:1487–1498. https://doi.org/10.1097/CCM.0b013e3182416f23.
9. Gill JR, Sheng ZM, Ely SF, Guinee DG, Beasley MB, Suh J, Deshpande C, Mollura DJ, Morens DM, Bray M, Travis WD, Taubenberger JK. 2010. Pulmonary pathologic findings of fatal 2009 pandemic influenza A/h1n1 viral infections. Arch Pathol Lab Med 134:235–243.
10. Shah NS, Greenberg JA, McNulty MC, Gregg KS, Riddell J, Mangino JE, Weber DM, Hebert CL, Marzec NS, Barron MA, Chaparro-Rojas F, Restrepo A, Hemmige V, Prasidthrathsint K, Cobb S, Herwaldt L, Raabe V, Cannavino CR, Hines AG, Bares SH, Antiporta PB, Scardina T, Patel U, Reid G, Mohazabnia P, Kachhdiya S, Le BM, Park CJ, Ostrowsky B, Robicsek A, Smith BA, Schied J, Bhatti MM, Mayer S, Sikka M, Murphy-Aguilu I, Patwari P, Abeles SR, Torriani FJ, Abbas Z, Toya S, Doktor K, Chakrabarti A, Doblecki-Lewis S, Looney DJ, David MZ. 2016. Bacterial and viral co-infections complicating severe influenza: incidence and impact among 507 U.S. patients, 2013–14. J Clin Virol 80:12–19. https://doi.org/10.1016/j.jcv.2016.04.008.
11. Hashimoto Y, Moki T, Takizawa T, Shiratsuchi A, Nakanishi Y. 2007. Evidence for phagocytosis of influenza virus-infected, apoptotic cells by neutrophils and macrophages in mice. J Immunol 178:2448–2457. https://doi.org/10.4049/jimmunol.178.4.2448.
12. Garten RJ, Davis CT, Russell CA, Shu B, Lindstrom S, Balish A, Sessions WM, Xu X, Skepner E, Deyde V, Okomo-Adhiambo M, Gubareva L, Barnes J, Smith CB, Emery SL, Hillman MJ, Rivailler P, Smagala J, de Graaf M, Burke DF, Fouchier RA, Pappas C, Alpuche-Aranda CM, López-Gatell H, Olivera H, López I, Myers CA, Faix D, Blair PJ, Yu C, Keene KM, Dotson PD, Boxrud D, Sambol AR, Abid SH, St George K, Bannerman T, Moore AL, Stringer DJ, Blevins P. 2009. Antigenic and genetic characteristics of swine-origin 2009 A (H1N1) influenza viruses circulating in humans. Science 325:197–201. https://doi.org/10.1126/science.1176225.
13. Safronetz D, Rockx B, Feldmann F, Belisle SE, Palermo RE, Brining D, Gardner D, Proll SC, Marzi A, Tsuda Y, LaCasse RA, Kercher L, York A, Korth MJ, Long D, Rosenke R, Shupert WL, Aranda CA, Mattoon JS, Kobasa D, Kobinger G, Li Y, Taubenberger JK, Richt JA, Parnell M, Ebihara H, Kawaoka Y, Katze MG, Feldmann H. 2011. Pandemic swine-origin H1N1 influenza A virus isolates show heterogeneous virulence in macaques. J Virol 85:1214–1223. https://doi.org/10.1128/JVI.01848-10.
14. Itoh Y, Shinya K, Kiso M, Watanabe T, Sakoda Y, Hatta M, Muramoto Y, Tamura D, Sakai-Tagawa Y, Noda T, Sakabe S, Imai M, Hatta Y, Watanabe S, Li C, Yamada S, Fujii K, Murakami S, Imai H, Kakugawa S, Ito M, Takano R, Iwatsuki-Horimoto K, Shimojima M, Horimoto T, Goto H, Takahashi K, Makino A, Ishigaki H, Nakayama M, Okamatsu M, Takahashi K, Warshauer D, Shult PA, Saito R, Suzuki H, Furuta Y, Yamashita M, Mitamura K, Nakano K, Nakamura M, Brockman-Schneider R, Mitamura H, Yamazaki M, Sugaya N, Suresh M, Ozawa M, Neumann G, Gern J, Kida H, Ogasawara K, Kawaoka Y. 2009. *In vitro* and *in vivo* characterization of new swine-origin H1N1 influenza viruses. Nature 460:1021–1025. https://doi.org/10.1038/nature08260.
15. Paquette SG, Banner D, Chi le TB, León AJ, Xu L, Ran L, Huang SSH, Farooqui A, Kelvin DJ, Kelvin AA. 2014. Pandemic H1N1 influenza A directly induces a robust and acute inflammatory gene signature in primary human bronchial epithelial cells downstream of membrane fusion. Virology 448:91–103. https://doi.org/10.1016/j.virol.2013.09.022.
16. Abramson JS, Lewis JC, Lyles DS, Heller KA, Mills EL, Bass DA. 1982. Inhibition of neutrophil lysosome-phagosome fusion associated with influenza virus infection *in vitro*. Role in depressed bactericidal activity. J Clin Invest 69:1393–1397. https://doi.org/10.1172/JCI110580.
17. Abramson JS, Giebink GS, Quie PG. 1982. Influenza A virus-induced polymorphonuclear leukocyte dysfunction in the pathogenesis of experimental pneumococcal otitis media. Infect Immun 36:289–296.
18. Abramson JS, Lyles DS, Heller KA, Bass DA. 1982. Influenza A virus-induced polymorphonuclear leukocyte dysfunction. Infect Immun 37: 794–799.
19. Abramson JS, Mills EL, Giebink GS, Quie PG. 1982. Depression of monocyte and polymorphonuclear leukocyte oxidative metabolism and bactericidal capacity by influenza A virus. Infect Immun 35:350–355.
20. Abramson JS, Parce JW, Lewis JC, Lyles DS, Mills EL, Nelson RD, Bass DA. 1984. Characterization of the effect of influenza virus on polymorphonuclear leukocyte membrane responses. Blood 64:131–138.
21. Abramson JS, Giebink GS, Mills EL, Quie PG. 1981. Polymorphonuclear leukocyte dysfunction during influenza virus infection in chinchillas. J Infect Dis 143:836–845. https://doi.org/10.1093/infdis/143.6.836.
22. Debets-Ossenkopp Y, Mills EL, van Dijk WC, Verbrugh HA, Verhoef J. 1982. Effect of influenza virus on phagocytic cells. Eur J Clin Microbiol 1:171–177. https://doi.org/10.1007/BF02019619.
23. Larson HE, Blades R. 1976. Impairment of human polymorphonuclear leucocyte function by influenza virus. Lancet i:283. https://doi.org/10.1016/S0140-6736(76)91407-0.
24. Larson HE, Parry RP, Gilchrist C, Luquetti A, Tyrrell DA. 1977. Influenza viruses and staphylococci in vitro: some interactions with polymorphonuclear leucocytes and epithelial cells. Br J Exp Pathol 58:281–288.
25. Ruutu P, Vaheri A, Kosunen TU. 1977. Depression of human neutrophil motility by influenza virus *in vitro*. Scand J Immunol 6:897–906. https://doi.org/10.1111/j.1365-3083.1977.tb00410.x.
26. Hartshorn KL, Liou LS, White MR, Kazhdan MM, Tauber JL, Tauber AI. 1995. Neutrophil deactivation by influenza A virus. Role of hemagglutinin binding to specific sialic acid-bearing cellular proteins. J Immunol 154:3952–3960.
27. Hartshorn KL, White MR. 1999. Influenza A virus up-regulates neutrophil

adhesion molecules and adhesion to biological surfaces. J Leukoc Biol 65:614–622.
28. Rothwell SW, Wright DG. 1994. Characterization of influenza A virus binding sites on human neutrophils. J Immunol 152:2358–2367.
29. Childs RA, Palma AS, Wharton S, Matrosovich T, Liu Y, Chai W, Campanero-Rhodes MA, Zhang Y, Eickmann M, Kiso M, Hay A, Matrosovich M, Feizi T. 2009. Receptor-binding specificity of pandemic influenza A (H1N1) 2009 virus determined by carbohydrate microarray. Nat Biotechnol 27:797–799. https://doi.org/10.1038/nbt0909-797.
30. Abramson JS, Wheeler JG, Parce JW, Rowe MJ, Lyles DS, Seeds M, Bass DA. 1986. Suppression of endocytosis in neutrophils by influenza A virus *in vitro*. J Infect Dis 154:456–463. https://doi.org/10.1093/infdis/154.3.456.
31. Cassidy LF, Lyles DS, Abramson JS. 1988. Synthesis of viral proteins in polymorphonuclear leukocytes infected with influenza A virus. J Clin Microbiol 26:1267–1270.
32. Zhang Z, Huang T, Yu F, Liu X, Zhao C, Chen X, Kelvin DJ, Gu J. 2015. Infectious progeny of 2009 A (H1N1) influenza virus replicated in and released from human neutrophils. Sci Rep 5:17809. https://doi.org/10.1038/srep17809.
33. Fujisawa H. 2008. Neutrophils play an essential role in cooperation with antibody in both protection against and recovery from pulmonary infection with influenza virus in mice. J Virol 82:2772–2783. https://doi.org/10.1128/JVI.01210-07.
34. Ivan FX, Tan KS, Phoon MC, Engelward BP, Welsch RE, Rajapakse JC, Chow VT. 2013. Neutrophils infected with highly virulent influenza H3N2 virus exhibit augmented early cell death and rapid induction of type I interferon signaling pathways. Genomics 101:101–112. https://doi.org/10.1016/j.ygeno.2012.11.008.
35. Colamussi ML, White MR, Crouch E, Hartshorn KL. 1999. Influenza A virus accelerates neutrophil apoptosis and markedly potentiates apoptotic effects of bacteria. Blood 93:2395–2403.
36. Engelich G, White M, Hartshorn KL. 2001. Neutrophil survival is markedly reduced by incubation with influenza virus and *Streptococcus pneumoniae*: role of respiratory burst. J Leukoc Biol 69:50–56.
37. Choi UY, Kang JS, Hwang YS, Kim YJ. 2015. Oligoadenylate synthase-like (OASL) proteins: dual functions and associations with diseases. Exp Mol Med 47:e144. https://doi.org/10.1038/emm.2014.110.
38. Li Y, Banerjee S, Wang Y, Goldstein SA, Dong B, Gaughan C, Silverman RH, Weiss SR. 2016. Activation of RNase L is dependent on OAS3 expression during infection with diverse human viruses. Proc Natl Acad Sci U S A 113:2241–2246. https://doi.org/10.1073/pnas.1519657113.
39. Morales DJ, Lenschow DJ. 2013. The antiviral activities of ISG15. J Mol Biol 425:4995–5008. https://doi.org/10.1016/j.jmb.2013.09.041.
40. Zhao C, Hsiang TY, Kuo RL, Krug RM. 2010. ISG15 conjugation system targets the viral NS1 protein in influenza A virus–infected cells. Proc Natl Acad Sci U S A 107:2253–2258. https://doi.org/10.1073/pnas.0909144107.
41. Tang Y, Zhong G, Zhu L, Liu X, Shan Y, Feng H, Bu Z, Chen H, Wang C. 2010. Herc5 attenuates influenza A virus by catalyzing ISGylation of viral NS1 protein. J Immunol 184:5777–5790. https://doi.org/10.4049/jimmunol.0903588.
42. Gerlach RL, Camp JV, Chu YK, Jonsson CB. 2013. Early host responses of seasonal and pandemic influenza A viruses in primary well-differentiated human lung epithelial cells. PLoS One 8:e78912. https://doi.org/10.1371/journal.pone.0078912.
43. Tate MD, Ioannidis LJ, Croker B, Brown LE, Brooks AG, Reading PC. 2011. The role of neutrophils during mild and severe influenza virus infections of mice. PLoS One 6:e17618. https://doi.org/10.1371/journal.pone.0017618.
44. Perrone LA, Plowden JK, García-Sastre A, Katz JM, Tumpey TM. 2008. H5N1 and 1918 pandemic influenza virus infection results in early and excessive infiltration of macrophages and neutrophils in the lungs of mice. PLoS Pathog 4:e1000115. https://doi.org/10.1371/journal.ppat.1000115.
45. Tate MD, Deng YM, Jones JE, Anderson GP, Brooks AG, Reading PC. 2009. Neutrophils ameliorate lung injury and the development of severe disease during influenza infection. J Immunol 183:7441–7450. https://doi.org/10.4049/jimmunol.0902497.
46. Narasaraju T, Yang E, Samy RP, Ng HH, Poh WP, Liew AA, Phoon MC, van Rooijen N, Chow VT. 2011. Excessive neutrophils and neutrophil extracellular traps contribute to acute lung injury of influenza pneumonitis. Am J Pathol 179:199–210. https://doi.org/10.1016/j.ajpath.2011.03.013.
47. Sakai S, Kawamata H, Mantani N, Kogure T, Shimada Y, Terasawa K, Sakai T, Imanishi N, Ochiai H. 2000. Therapeutic effect of anti-macrophage inflammatory protein 2 antibody on influenza virus-induced pneumonia in mice. J Virol 74:2472–2476. https://doi.org/10.1128/JVI.74.5.2472-2476.2000.
48. Bordon J, Aliberti S, Fernandez-Botran R, Uriarte SM, Rane MJ, Duvvuri P, Peyrani P, Morlacchi LC, Blasi F, Ramirez JA. 2013. Understanding the roles of cytokines and neutrophil activity and neutrophil apoptosis in the protective versus deleterious inflammatory response in pneumonia. Int J Infect Dis 17:e76–e83. https://doi.org/10.1016/j.ijid.2012.06.006.
49. Walters KA, D'Agnillo F, Sheng ZM, Kindrachuk J, Schwartzman LM, Kuestner RE, Chertow DS, Golding BT, Taubenberger JK, Kash JC. 2016. 1918 pandemic influenza virus and *Streptococcus pneumoniae* coinfection results in activation of coagulation and widespread pulmonary thrombosis in mice and humans. J Pathol 238:85–97. https://doi.org/10.1002/path.4638.
50. Kash JC, Xiao Y, Davis AS, Walters KA, Chertow DS, Easterbrook JD, Dunfee RL, Sandouk A, Jagger BW, Schwartzman LM, Kuestner RE, Wehr NB, Huffman K, Rosenthal RA, Ozinsky A, Levine RL, Doctrow SR, Taubenberger JK. 2014. Treatment with the reactive oxygen species scavenger EUK-207 reduces lung damage and increases survival during 1918 influenza virus infection in mice. Free Radic Biol Med 67:235–247. https://doi.org/10.1016/j.freeradbiomed.2013.10.014.
51. Robinson KM, McHugh KJ, Mandalapu S, Clay ME, Lee B, Scheller EV, Enelow RI, Chan YR, Kolls JK, Alcorn JF. 2014. Influenza A virus exacerbates *Staphylococcus aureus* pneumonia in mice by attenuating antimicrobial peptide production. J Infect Dis 209:865–875. https://doi.org/10.1093/infdis/jit527.
52. Zurbach KA, Moghbeli T, Snyder CM. 2014. Resolving the titer of murine cytomegalovirus by plaque assay using the M2-10B4 cell line and a low viscosity overlay. Virol J 11:71. https://doi.org/10.1186/1743-422X-11-71.
53. Klimov A, Balish A, Veguilla V, Sun H, Schiffer J, Lu X, Katz JM, Hancock K. 2012. Influenza virus titration, antigenic characterization, and serological methods for antibody detection. Methods Mol Biol 865:25–51. https://doi.org/10.1007/978-1-61779-621-0_3.
54. Kobayashi SD, Voyich JM, Buhl CL, Stahl RM, DeLeo FR. 2002. Global changes in gene expression by human polymorphonuclear leukocytes during receptor-mediated phagocytosis: cell fate is regulated at the level of gene expression. Proc Natl Acad Sci U S A 99:6901–6906. https://doi.org/10.1073/pnas.092148299.
55. Benjamini YH, Yosef H. 1995. Controlling the false discovery rate: a practical and powerful approach to multiple testing. J R Stat Soc B Stat Methodol 57:289–300.
56. Murray RJ, Robinson JO, White JN, Hughes F, Coombs GW, Pearson JC, Tan HL, Chidlow G, Williams S, Christiansen KJ, Smith DW. 2010. Community-acquired pneumonia due to pandemic A(H1N1)2009 influenza virus and methicillin resistant *Staphylococcus aureus* co-infection. PLoS One 5:e8705. https://doi.org/10.1371/journal.pone.0008705.
57. Shaw ML, Stone KL, Colangelo CM, Gulcicek EE, Palese P. 2008. Cellular proteins in influenza virus particles. PLoS Pathog 4:e1000085. https://doi.org/10.1371/journal.ppat.1000085.
58. Graves SF, Kobayashi SD, Braughton KR, Whitney AR, Sturdevant DE, Rasmussen DL, Kirpotina LN, Quinn MT, DeLeo FR. 2012. Sublytic concentrations of *Staphylococcus aureus* Panton-Valentine leukocidin alter human PMN gene expression and enhance bactericidal capacity. J Leukoc Biol 92:361–374. https://doi.org/10.1189/jlb.1111575.
59. Lu T, Porter AR, Kennedy AD, Kobayashi SD, DeLeo FR. 2014. Phagocytosis and killing of *Staphylococcus aureus* by human neutrophils. J Innate Immun 6:639–649. https://doi.org/10.1159/000360478.